



Department of Electrical and Computer Engineering

ELECTENG 701 Wireless Communications

Wireless Systems

Andrew Austin

This part of the course focuses on *wireless systems* and is divided into four modules:

- Cellular Mobile Systems;
- Frequency Reuse, Outage Probability and Interference;
- Space Diversity and MIMO; and
- Wireless System Performance Estimation.

These notes are supported by a series of delivered lectures, problem sheets and worked examples.

1 Cellular Mobile Systems

1.1 Broadcast Systems and Radio Telephones

Before discussing cellular systems, it is useful to make the comparison with *broadcast* systems, e.g., analog/digital TV and radio. In wireless broadcast systems communication is typically one-directional (half-duplex), i.e., most users only have a radio/TV *receiver*, not a transmitter. In these systems the same ‘message’ signal is typically sent to each user (multiple TV/radio channels are transmitted with different carrier frequencies), and the number of users ‘connected’ usually does not have an impact on the system design. Accordingly, the main concern for broadcast systems is ensuring sufficient *coverage*, i.e., the signal level at a location is sufficiently above the noise-floor. Typically transmitting antennas are mounted atop hills, buildings or towers to ensure a large coverage area. Furthermore, frequencies in the VHF (30–300 MHz) and lower UHF bands (300–3000 MHz) are used

to reduce the impact of diffraction losses. *Co-channel interference* (caused by signals transmitted on the same frequency) is usually not an issue with broadcast systems. Frequencies are often *reused*, i.e., the same frequency is used for another channel and transmitted from another antenna, some distance away—e.g., 92.6 MHz is used in Auckland for ‘Radio NZ Concert’, while in the Bay of Plenty 92.6 MHz is used for ‘The Sound’—but in broadcast systems the large separation distance between co-channel transmitters usually ensures low levels of interference.

1.1.1 Bi-directional Communications

For bi-directional communications, where each user wants to send/receive *different* message signals, it is necessary to assign a different frequency (or time-slot) to each user. This was the basis behind early radio-telephones, which were first made available for public¹ use in the USA in 1946. These systems operated at 152 MHz, and as a single transmitter was used to cover an entire metropolitan area, capacity was extremely limited. It is also important to note that as these systems required an additional frequency channel (compared to broadcast systems) to enable simultaneous transmission and reception (termed *full-duplex*). These early radio telephony systems used frequency modulation (FM) and were extremely spectrally inefficient (with channel bandwidths in excess of 100 kHz, despite the voice signal only occupying 3 kHz!), largely due to the difficulties in mass producing suitable analog filters and other components.

1.1.2 Mobile Telephones

By the mid 1970s, channel bandwidths were reduced to 30 kHz and these systems could be connected to existing phone networks. It is important to note that while these systems were termed ‘mobile telephones’, the power consumption requirements usually meant that most were installed in vehicles. Nevertheless, public demand remained high, for example, in 1976 while the Bell Mobile Phone system for New York City could only support 543 users², over 3500 people were on the waiting list [1, p. 4]. The main limiting factor in these early networks was the ‘shortage’ of radio spectrum. It is important to note that in most countries, allocation and use of frequencies is regulated by the government (in NZ this is currently the Radio Spectrum Management Unit, part of the Ministry of Business, Innovation and Employment).

1.2 The Concept of Cellular Systems

Clearly, deploying mobile communication systems using a broadcast approach could not meet the capacity demands and a major redesign was necessary. The first *cellular systems* were deployed in several USA cities in

¹The first (civilian) land-mobile radio communication systems were installed in the 1920s—initially for police departments in the United States—however, these were not available to the general public.

²Note also that while Bell sold 543 ‘subscriptions’, only **12 users** could simultaneously make/receive mobile phone calls in New York City!

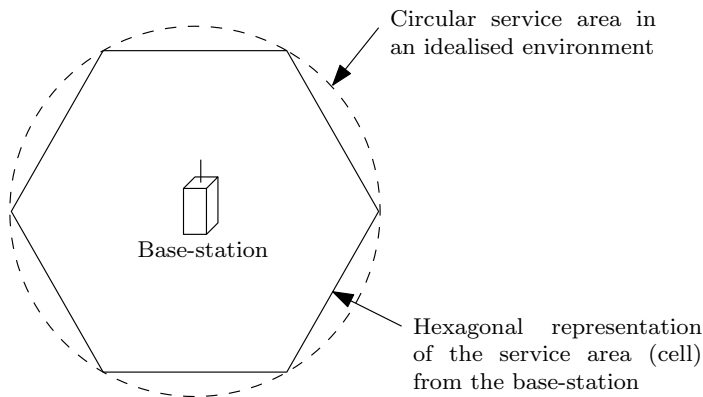


Fig. 1: Hexagonal representation of the service area from a base-station. Adapted from [2, p. 4].

1979 (although the concept had been proposed and developed from the late 1960s) and in Scandinavia in 1981³. The cellular concept is similar to the reallocation/reuse of FM radio channels in different parts of the country, except the reuse happens on a much smaller scale—in some cases the co-channel transmitters can be only 100s of metres apart in dense urban environments. The main difference from broadcast systems is the replacement of the single (high-power) transmitter with many low-power transmitters that only provide coverage to a small portion of the original region. These small regions are termed *cells* and each low-power transmitter is termed a *base-station*. Each base-station is allocated a *portion* of total number of channels available to the system. The base-stations in adjacent cells are allocated different sets of channels, i.e., immediately adjacent cells will not interfere with each other. As the total number of channels is limited, frequencies are reused in non-adjacent cells. Cellular systems also have the advantage that within a single cell we can create additional smaller cells in regions of high-user density by reusing other sets of channels—this is termed *cell-splitting*.

1.2.1 Frequency Reuse

By reusing the frequencies in nearby base-stations a much higher degree of coverage can be obtained, without requiring any further spectrum. However, this frequency reuse leads to co-channel interference. In order to minimise the levels of interference, the location of co-channel base-stations must be carefully planned *before* the system is deployed. In order to optimise deployments reliable estimates of the signal strength from both the ‘desired’ and ‘interfering’ base-stations are required across the cell. Given the variations in terrain height and surrounding environmental clutter, such as buildings, detailed propagation modelling is required, and is often validated with experimental measurements. Despite the complexity of the propagation processes, it is typical to depict the coverage area of a cell as hexagonal,

³These systems were also incompatible with each other, a common theme that continues to be an issue with wireless communication systems.

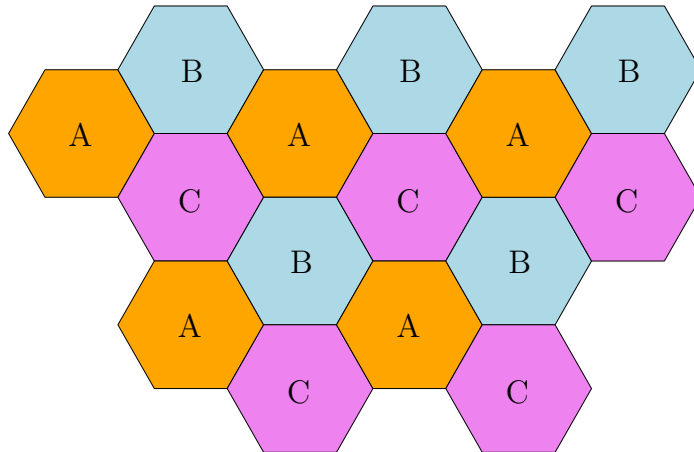


Fig. 2: Allocation of three sets of channel frequencies in a generalised cellular system.

as shown in Fig. 1. The hexagonal shape closely approximates a circular radiation pattern (i.e., free space propagation and an omni-directional antenna) and allows tessellation without leaving gaps or creating overlapping regions and is thus a useful model for planning frequency allocations. For example, Fig. 2 shows a cellular system frequency allocation with three sets of non-overlapping channels, denoted by A, B and C; we will go into this problem in more detail in module 2.

1.2.2 Cell Sizes

The size of the cell depends on the expected user density, and to improve capacity, the physical region covered by each cell can be reduced; accordingly lower power is required from the base-stations. The optimal allocation of frequency channels—particularly in regions with high user density, such as urban/metropolitan areas and within buildings—remains a challenge for modern cellular systems. Fig. 3 shows a representation of some typical cell sizes:

- *Macro-cells* are designed to provide outdoor coverage for rural, sub-urban and urban environments. A typical coverage area is between 1–10 km, and accordingly the antennas are usually mounted above the surrounding terrain and buildings.
- To provide better coverage for users in urban environments, a large macro-cell can be split into several *micro-cells*. In this case the base-station typically provides coverage over a range of less than 1 km, and the antennas are usually mounted at street level.
- However, regions with high traffic density (e.g. train-stations and airports) are not well serviced by macro- or micro-cells. To extend coverage to these regions, pico-cells—typically with a maximum range between 20–200 m—can be deployed. Achieving adequate coverage

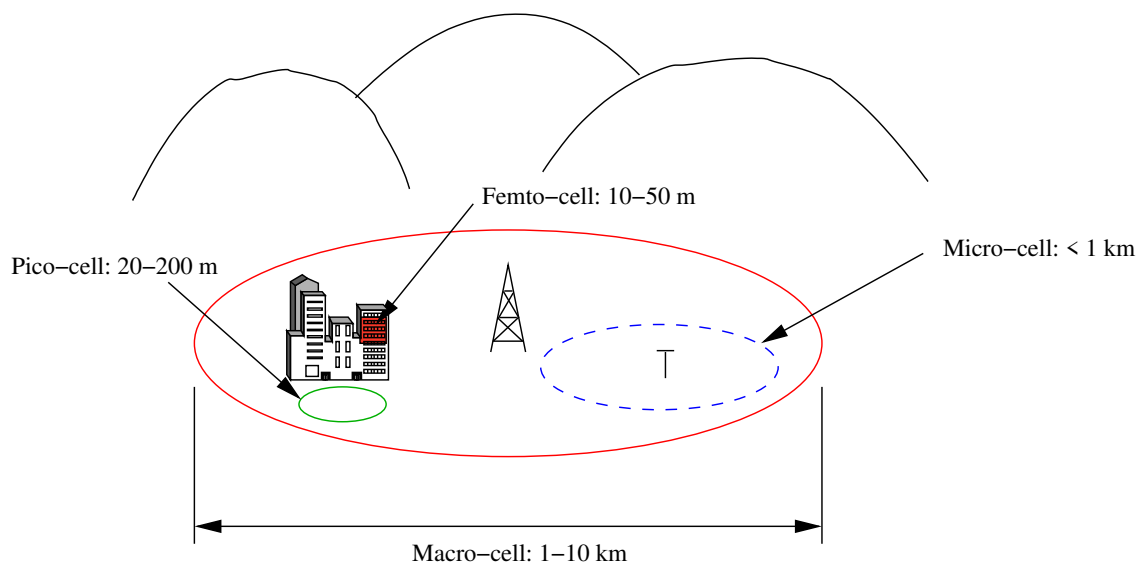


Fig. 3: Illustration of the different cell sizes in a typical cellular system. This diagram also illustrates the principle of *cell-splitting*, i.e., reuse of frequencies within a cell to increase capacity.

and reliable system performance within buildings with micro- and pico-cells is particularly challenging as, though the users are relatively stationary, the traffic density can be extremely high. Furthermore, because the transmitters are generally located outside, large penetration losses are often encountered when propagating a signal into a building.

- To improve cellular system performance within buildings, a further decrease in the cell size has been suggested. *Femto-cells* have a maximum range between 10–50 m and are designed to be located indoors to provide improved coverage within small buildings, or across several floors of larger buildings. Femto-cells still operate in the licensed portions of the frequency spectrum; however, as the frequency reuse distances are generally smaller this leads to increased levels of co-channel interference.

One of the challenges with cellular systems is the need to seamlessly *hand-over* a ‘call’ when a user moves from one cell to another. These can be categorised as ‘hard’ or ‘soft’: in a hard hand-over the original cell releases the call once the signal level drops below a threshold, without checking if the new cell has an available channel; by contrast in a soft hand-over the call is simultaneously supported by both cells until the transfer is confirmed.

1.3 The Evolution of Wireless Systems and Standards

1.3.1 Cellular Systems

The cellular industry has applied the term *generation* to describe successive advances in mobile communications. In this section we will briefly outline

the key differences and similarities between cellular systems from the first generation (1G) to the current fourth generation (4G). Table 1 outlines **some** of the standards and technologies used in 1G–4G systems.

- 1G systems⁴ used FM to modulate voice signals onto an RF carrier. Multiple users can be supported as each user is assigned a different frequency channel to transmit/receive on, this is termed *frequency division multiple access* (FDMA). In the most widely used 1G system, AMPS (Advanced Mobile Phone System)—which was first deployed in NZ in 1987 by Telecom—the bandwidth of each channel was 30 kHz, which could support three users simultaneously. 1G cell phones were correspondingly large and bulky to accommodate the analog components, in particular the filters required to reduce interference from adjacent frequency channels. Digital data transmissions could be supported in 1G, but was only used for sending system information, e.g., user-IDs and connection status.
- 2G systems were digital, but were primarily designed for voice transmissions, i.e., the voice signal was first sampled, quantised and converted into a digital message signal (however short messages, e.g., TXT messages could also be sent). There were two main competing standards for 2G: GSM⁵ from Europe and IS-95⁶ from the USA. Both of these systems are still supported in many countries as legacy standards. The underlying technologies are very different: GSM uses time-division multiple-access (TDMA) to separate the users. In TDMA systems each user gets a particular time slot on which they receive/send signals. Accordingly GSM needs a reasonable amount of overhead to ensure all users and devices remain synchronised, otherwise inter-user interference can result. The actual data for each user is simply encoded using phase-shift-keying, e.g., BPSK or QPSK.

IS-95 by contrast uses a very different approach to separate the users, called *code-division multiple access* (CDMA). Unlike FDMA or TDMA, in CDMA systems all users transmit simultaneously and over the same frequency range. In FDMA or TDMA systems this would create significant interference and would prevent any messages from being received. However, CDMA assigns a unique *spreading code* to each user in the system. These codes are orthogonal to each other, so that each receiver can recover its message by correlating the incoming signal with a locally generated version of the spreading code. The other users in CDMA system are uncorrelated and will thus appear as noise.

- Similar to 2G, there were two main 3G standards: CDMA-2000 from the USA and UMTS (Universal Mobile Telecommunications Service) from Europe. In New Zealand, both networks were originally supported by Telecom (now Spark) and Vodafone respectively, however,

⁴Note that at the time no one called these 1G systems, the naming convention was applied retrospectively.

⁵GSM originally stood for *Groupe Special Mobile*, but this acronym was later converted to *Global System for Mobile*.

⁶Interim Standard 95, which was developed by Qualcomm in 1995.

Spark eventually switched in 2012 to UTMS. Both standards use CDMA to separate the users, however there are significant differences in the bandwidths and carrier frequencies, making the systems mutually incompatible. 3G systems were designed around carrying data traffic, with voice treated largely as ‘another data stream’. The data rates of 3G systems were sufficient to deliver the internet to mobile phones, which has been the enabling factor in the growth of mobile applications and services, e.g., Uber, Skype, Spotify, etc.

- Currently there is one 4G standard that the cellular industry has coalesced around—LTE-A (Long Term Evolution Advanced). LTE-A is designed primarily to carry data traffic at considerably higher data-rates than 3G systems. The users in an LTE-A system are separated with Orthogonal Frequency Division Multiple Access (OFDMA), which is designed to limit the amounts of interference, but poses some constraints on the required synchronisation accuracy. LTE-A systems are supported world-wide, however there are over 40 different channels spread across the spectrum from 700 MHz–2100 MHz, which complicates the design of the mobile devices and base-stations.

1.3.2 Wireless Computer Networks

The proliferation of cellular systems has been paralleled by the development of wireless computer networks operating in unlicensed portions of the spectrum. Wireless Local Area Networks (WLAN) are often deployed within buildings to provide wireless connectivity to existing networks or the internet. The current generation of WLANs are based on the IEEE 802.11 ‘family’ of standards, and were originally introduced in the mid 1990s. Successive improvements—e.g., IEEE 802.11b (CDMA, 2.45 GHz), 802.11a (OFDM, 5.8 GHz), 802.11g (OFDM, 2.45 GHz) and 802.11n (OFDM/MIMO, 2.45 GHz)⁷—have seen a steady increase in performance, although in comparison to contemporary wired networking, the maximum data rates are still relatively low. Moreover, systems operating in the unlicensed frequency bands are prone to interference from other systems and devices operating in close physical proximity.

The IEEE 802.11 standard outlines communication protocols for WLANs operating in the unlicensed portions of the 2.4 GHz industrial, scientific and medical (ISM) frequency band, and the 5.8 GHz unlicensed national information infrastructure (U-NII) band. Systems supporting the 802.11 standard are widely deployed within buildings to provide wireless connectivity. Fig. 4 shows how the 802.11 standard divides the 2.4 GHz band into 11 channels⁸ with 20 MHz bandwidth/channel. Each channel can support multiple users simultaneously by separating the users with different spreading codes (e.g., CDMA) or, in frequency with orthogonal sub-carriers (e.g., OFDM). It should be noted that there is considerable overlap between adjacent channels, e.g., in the 2.4 GHz band shown in Fig. 4, only

⁷Abbreviations—CDMA: code-division multiple-access; OFDM: orthogonal frequency-division multiplexing; MIMO: multiple-input multiple-output.

⁸The USA version of the standard divides the 2.4 GHz band into 11 channels; in other areas of the world up to 14 channels can be used.

Table 1: Selected Cellular Systems and Standards from 1G to 4G. Adapted from [3].

Name	AMPS	GSM	IS-95	CDMA-2000	UTMS/W-CDMA	LTE-A
Generation	1	2	2	3	3	(3.9) 4
Year of introduction and origin	1983 USA	1992 Germany	1993 USA	2002 USA	2002 Europe	2009 Europe
Region of use	USA	Europe, India, AU/NZ	USA, HK, ME AU/NZ	USA, AU/NZ	Europe, AU/NZ	World-wide
Frequency band						
Up-link (MHz)	824-859	890-915, 1850-1910	824-849, 1850-1910	1850-1910	1920-1980	Depends
Down-link (MHz)	869-894	935-960, 1930-1950	869-894, 1930-1990	1930-1990	2110-2170	on country
Multiple access scheme	FDMA	TDMA	CDMA	CDMA	CDMA	OFDMA/MIMO
BW/Channel	30 kHz	200 kHz	1.25 MHz	1.25-15 MHz	5-20 MHz	1.4-20 MHz
Modulation Type	FM	GMSK	QPSK	QPSK, BPSK	QPSK, BPSK	OFDM
Max. power						
Base-station	20 W	320 W	1.64 kW	1.64 kW	unspecified	unspecified
Mobile	4 W	8 W	6.3 W	2 W	1 W	1 W
Users/channel	3	8	63	253	250	200
Data-rate	19.2 kbps	22.8 kbps	19.2 kbps	1.5 kbps-2 Mbps	100 kbps-2 Mbps	300 Mbps

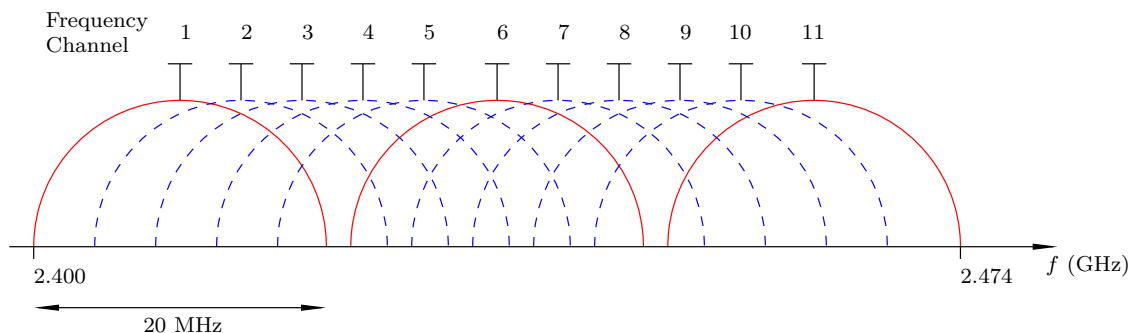


Fig. 4: Graphical representation of the 2.4 GHz frequency channels in the 802.11 standard. Each channel can support multiple users by separating them via CDMA or OFDM (adapted from [4, pp. 679–680]). The three channels identified in red do not overlap in frequency, and hence do not interfere with each other.

three channels (1, 6 and 11, identified in red) do not overlap in frequency. Therefore, when more than three channels are allocated to base-stations, frequencies are reused and varying levels of adjacent-channel interference could arise. Determining the optimal location of co-channel base-stations within buildings remains a challenge.

1.4 The Future of Cellular Systems

There are several directions that contemporary cellular and WLAN systems are heading in response to the increasing demand and ‘user’ density. While there are currently no standards for 5G systems, several industry groups have defined requirements that a 5G standard *should* achieve [5], in particular:

- increased data rates compared to 4G, with 10 Mbits/s for 10k+ users; 100 Mbits/s in urban areas and over 1 Gbit/s within buildings;
- improved spectral efficiency and coverage;
- latency of the air-interface below 1 ms and end-to-end latency of the system below 5 ms; and
- provision for 100,000s of wireless sensors.

Some of these requirements can be met by optimising existing systems, however, there is an increasing view that new air-interfaces and technology are required to meet the demand for cellular services. Convergence between cellular and IEEE 802.11 standards is also being discussed, however it is likely these will still be separate for another generation. This section will give an overview of some of the new technologies that have been proposed for 5G cellular systems and outlines some of the significant research challenges that remain.

1.4.1 Millimetre-Wave Systems

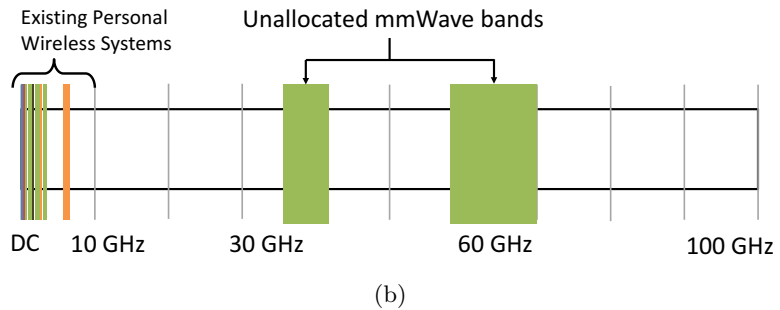
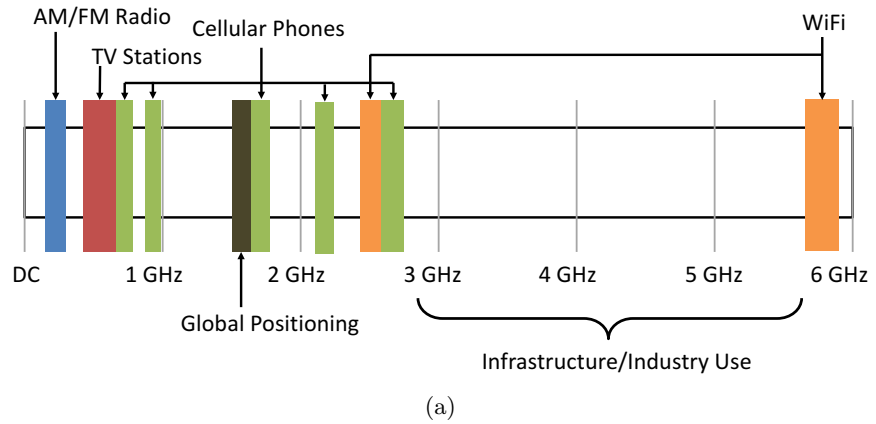


Fig. 5: (a) Current spectrum allocations for wireless personal communication systems operating below 6 GHz. (b) Currently unallocated spectrum in the mmWave bands.

As shown in Fig. 5(a) most wireless communication systems in use today operate in frequency bands below 6 GHz. These frequencies are becoming increasingly crowded, resulting in small channel allocations and significant congestion. For example, the widely used 2.4 GHz ISM band provides a mere 100 MHz of contiguous spectrum. Moreover, this spectrum is unlicensed and the spectral resource must be shared with an increasing number of other users, leading to considerable interference and substantially reduced data transmission rates. One solution to this spectral shortage problem is to move to higher frequencies where considerably more spectrum is available. In particular, recent advances in circuit technology are allowing the realisation of analog frontends for millimetre-wave (mmWave) frequencies between 30 GHz and 300 GHz, making abundant unused spectrum accessible, as depicted in Fig. 5(b). Technologies that use mmWave frequencies between 60–70 GHz are attracting considerable interest, as large bands of contiguous spectrum are available for use in a number of countries, including New Zealand. The large bandwidths (up to 8 GHz) available at 60 GHz have the potential to deliver short-range outdoor and indoor wireless systems with data-rates comparable to wired Ethernet systems.

Moving from sub-6 GHz to mmWave frequency bands increases the carrier frequency and channel bandwidth by over an order of magnitude, presenting considerable technical challenges—not least in the design of systems and the digital hardware required to process the high data-rate signals—but perhaps most importantly, the physics of the radio channel are significantly different, and propagation models developed for lower frequencies are inapplicable. There have been few reported models to characterise realistic mmWave propagation channels, and these have largely focused on simplified environments. In particular, there is increased propagation loss proportional to the square of the carrier frequency; and reduced diffraction around objects in the environment, leading to less coverage in shadowed regions. To overcome the increased propagation loss at mmWave frequencies, the use of highly directional antennas to focus the power has been proposed. These antennas provide a very narrow ‘pencil’ beam, and reception is only possible when the receiver is positioned within the beam. However, a wireless system is also expected to provide coverage at ‘all’ locations, and to users (and devices) that are moving. Accordingly, current research has focused on developing reconfigurable high-gain antennas for mmWave systems, where the position and size of the beam can be electronically controlled by altering the phase of the radiating elements. It is important to note that scaling-down the physical size of antennas designed for sub-6 GHz systems is not feasible as the conduction loss increases exponentially with frequency, and at mmWave frequencies most of the ‘transmitted’ power will not be radiated from the antenna, but will be lost to heat on the metal surface of the antennas and in the associated feeding networks.

1.4.2 True Full-Duplex

Fig. 6(a) shows a generalised cellular base-station transmitting to a mobile device. Practically all wireless systems in use today operate in half-duplex mode: to transfer information in both directions two communicating transceivers either take turns to use the radio channel—time-division duplex, as shown in Fig. 6(b)—or divide it into two disjoint frequency bands—frequency-division duplex, as shown in Fig. 6(c). As depicted in Fig. 6(d), in full-duplex mode, both transceivers simultaneously receive and transmit in the same frequency band. An immediate advantage of full-duplex operation is the effective doubling of the spectral efficiency, which is of considerable interest 5G cellular systems. Furthermore full-duplex links would greatly simplify resource allocation and spectrum management, reducing the overhead for ad-hoc and self-organising systems, such as wireless sensor networks.

One of the main challenges to realising full-duplex systems is the presence of strong self-interference, i.e., the signal power from the transceiver’s own transmitter is many orders of magnitude larger than the desired signal from the other transceiver. In theory, as the transmitted signal is ‘known’ within the transceiver, the resulting self-interference can be ‘subtracted’ off completely, leaving only the desired signal. Only with recent advances in digital systems design, analog and digital signal processing techniques and reconfigurable radio frequency hardware have implementations of full-

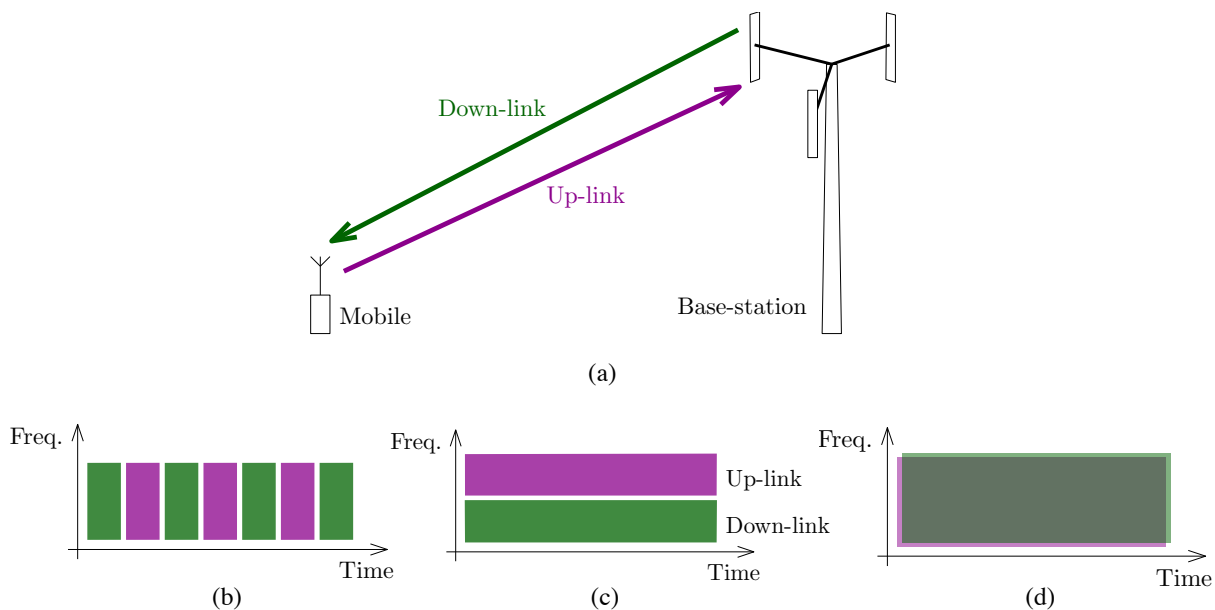


Fig. 6: (a) Identification of the up-link and down-link channels in a cellular system; (b) time-division duplexing; (c) frequency division duplexing; (d) ‘true’ full-duplex.

duplex systems been reported. While state-of-the-art full-duplex systems can achieve up to 80 dB self-interference suppression, all the reported implementations have been for narrowband systems operating with very low power. Scaling these results to practical transmit powers and bandwidths remains an active area of research.

1.4.3 Massive MIMO

Wireless multiple-input multiple-output (MIMO) systems use multiple antennas on the transmitter and receiver, as shown in Fig. 7. In a MIMO system with N antennas connected to both the transmitter and receiver, the capacity (and corresponding data-rates) can theoretically be increased by a factor on N . MIMO systems achieve this significant increase by exploiting the observation that the *correlation* between the signals received on multiple antennas decreases as the separation distance between these antennas is increased. Essentially this means that if we place our antennas sufficiently far apart the instantaneous channel response between any pair of transmitting/receiving antennas can be considered statistically independent. Generally to yield the theoretical improvement the number of antennas on the transmitter and receiver need to be the same (or nearly the same), which tends to limit the application of MIMO for hand-held devices. We will consider the conditions under which MIMO systems can successfully operate in more detail in Module 3.

Massive MIMO is a proposed technology that uses a large number (e.g.,

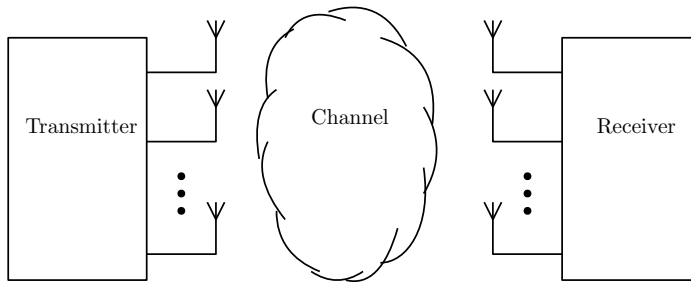


Fig. 7: High-level depiction of a MIMO system, with multiple-input and multiple-output antennas.

64–256) of antennas on the transmitter side to create directional ‘beams’ that can be steered to individual devices [6]. As the beams are very narrow there is potentially less interference. It should be noted that the user devices do *not* require multiple antennas. The challenges with massive MIMO is that it requires considerable signal processing to produce the necessary beams (which along with the additional antennas and feeding networks also increases the power consumption at the base-station) which must also be responsive to user movement and shadowing, e.g., if the user walks behind a building. Many cellular companies (including Spark NZ) are currently conducting field trials using massive MIMO technology in dense urban environments.

1.4.4 The Internet of Things

While mmWave, full-duplex, and massive MIMO technologies are intended to ‘solve’ the data-rate and spectral efficiency problems in the next generation of cellular and WLAN systems, there is also a need to develop wireless communication systems that can support the many hundreds of thousands of devices in the *Internet-of-Things* (IoT). In particular, these devices are not expected to transmit/receive large amounts of data and so will not require high-speed wireless technology. However, many of these devices will be battery/solar powered, so there will be a need to develop wireless technologies that have very low energy consumption in order to maximise the life-time of the network. Novel routing protocols that allow messages to be relayed on short-hops (thereby requiring less energy than a transmission directly to a base-station) are also an active area of research.

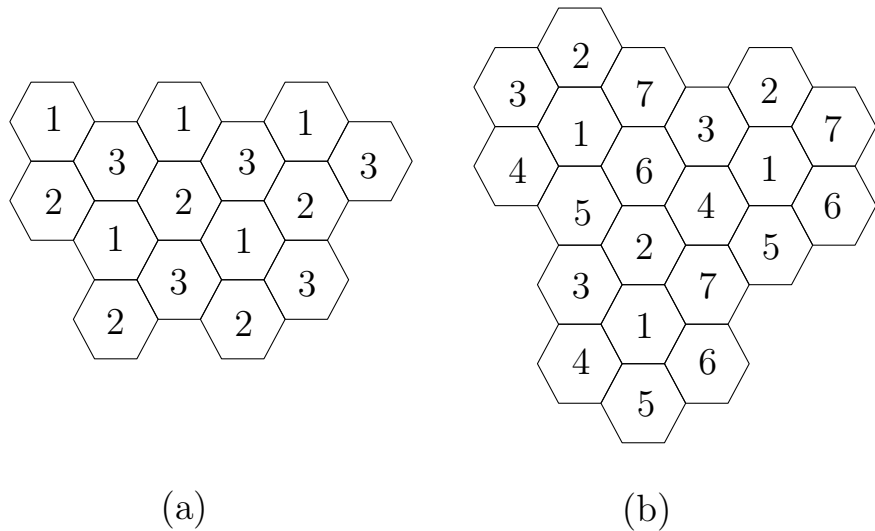


Fig. 8: Reuse patterns for (a) cluster size of 3; and (b) cluster size of 7.

2 Frequency Reuse, Interference and Outage Probability

In a cellular system sets of channel frequencies are reused⁹ in nearby cells in order to provide greater capacity (i.e., more users can be supported). Frequency reuse creates co-channel interference, reducing system performance. This section outlines how we can choose suitable reuse geometries that maximise the separation distances between co-channel cells for an *ideal* cellular system, i.e., one where the cellular coverage area can be approximated as a regular hexagon.

2.1 Cellular Reuse Geometries

The total number of frequency channels in a cellular system is fixed and depends on the total bandwidth available (purchased by the cellular operator) and the bandwidth required for each user. For example, if we assume a system operating in the 700–800 MHz band, where each user requires a 1 MHz channel, we have up to 100 frequency channels¹⁰ to allocate to each cell. In the extreme case, we could allocate each cell all 100 channels: this would allow high capacity (i.e., 100 users could connect to each cell), however, as all 100 frequency channels would be reused in adjacent cells, this would lead to very poor interference performance. Similarly, another extreme case would be to allocate each cell 1 channel: while this would result in a large reuse distance and minimal interference, each cell could only support 1 user!

⁹In this analysis we will restrict discussion to frequency reuse, i.e., FDMA systems, but similar time-slot reuse schemes are also needed for TDMA systems.

¹⁰In reality this number would be smaller than 100 due to the need for guard-bands.

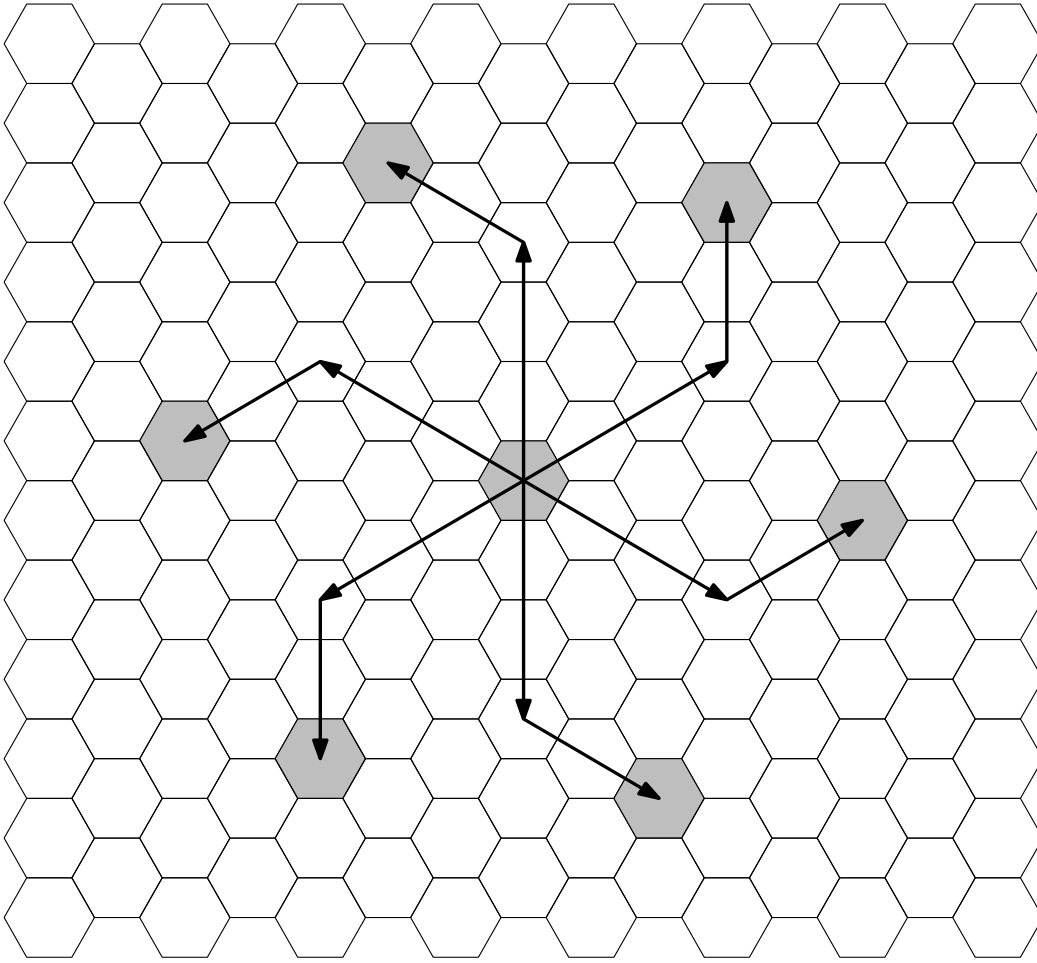


Fig. 9: The use of shift parameters to determine co-channel cells, $i = 3$, $j = 2$. Adapted from [2, p. 203].

2.1.1 Cluster size

The *cluster size* is the number of cells in the reuse pattern. Fig. 8(a) and (b) show examples of three- and seven-cell reuse patterns, i.e., cluster sizes of 3 and 7. For both these cases, all the co-channel base-stations are placed as far apart as possible, i.e., the *reuse distance* is maximised.

2.1.2 Shift Parameters

To determine suitable reuse patterns on a regular hexagonal grid we can use *shift parameters*, i and j . From any reference cell, the nearest co-channel cells can be found by moving out i cells from the reference cell in any of the six possible directions, turning anti-clockwise¹¹ and moving out a further j

¹¹Clockwise turns are also possible, it makes no difference as long as these are applied consistently

Table 2: Relationship between shift parameters, cluster size and reuse distance. Taken from [2, p. 204].

Shift Parameters		Cluster Size	Reuse Distance
i	j	$N = i^2 + ij + j^2$	$\frac{D}{R} = \sqrt{3N}$
0	1	1	1.73
1	1	3	3
0	2	4	3.46
1	2	7	4.58
0	3	9	5.12
2	2	12	6
1	3	13	6.24
0	4	16	6.93
2	3	19	7.55
1	4	21	7.94

cells [2, pp. 202–203]. For example, Fig. 9 illustrates the procedure for the shift parameters $i = 3$, $j = 2$. This process can be repeated until all the cells in the system have been allocated a set of channels.

The relationship between the cluster size, N , and the shift parameters i and j is,

$$N = i^2 + ij + j^2. \quad (1)$$

Note that as i and j are integers only certain cluster sizes are possible. Clearly systems with larger cluster sizes will have a greater frequency reuse distance (resulting in reduced interference), but there will be fewer channels available per cell. Based on the hexagonal geometry, it is possible to show that the reuse distance D is related to the radius of the cell R , by

$$\frac{D}{R} = \sqrt{3N}. \quad (2)$$

The cluster size thus determines the reuse distance, and several examples are presented in Table 2.

2.2 Interference

The performance of wireless systems is largely limited by interference from other systems (and devices) operating over the same frequency bands. Sources of interference in a cellular system include:

- Co-channel interference arising from base-stations and devices operating on the same frequency bands (i.e., frequency reuse);
- Adjacent-channel interference arising from imperfect filtering or intermodulation distortion IMD products; and
- Non-cellular systems which inadvertently leak energy into cellular bands through IMD.

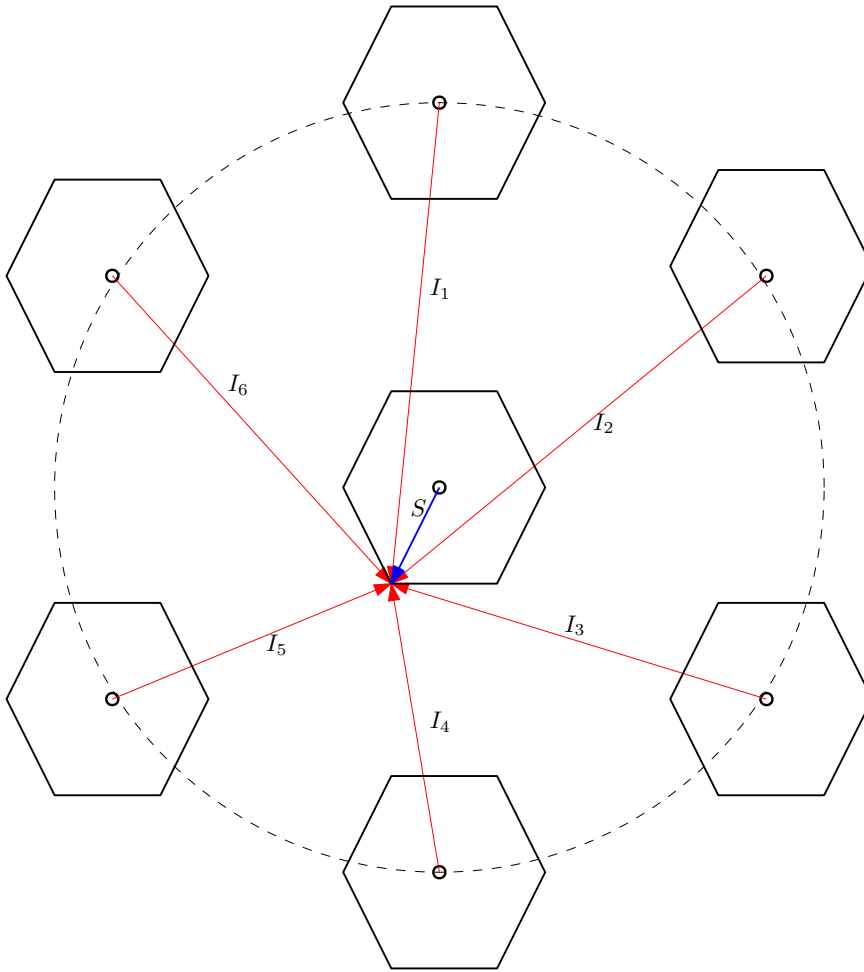


Fig. 10: Co-channel interference from the first layer of interfering cells. Adapted from [1, p. 41].

Unlike thermal noise, co-channel interference cannot be combatted by increasing the transmission power, as this increases the interference to neighbouring co-channel cells.

2.2.1 Signal-to-Interference Ratio

It is assumed that users in a cellular system will connect to the base-station from which the strongest power is received; the signal that is received from this base-station is termed the *desired* signal. Assuming identical channel conditions and that all base-stations transmit with the same power, the desired base-station will usually be one that is physically closest to the mobile. All other *co-channel* base-stations will thus appear as interference. The signal-to-interference ratio (SIR) for a mobile receiver on the down-link

channel can thus be expressed as

$$SIR = \frac{S}{C \sum_{i=1} I_i} \quad (3)$$

where S is the signal power from the desired base-station and I_i is the signal power from the i -th co-channel interfering base-station, when it is assumed there are C interfering base-stations in total. In most cases, we can approximate the total co-channel interference by considering only the first layer of interfering cells. Fig. 10 shows a diagram of the nearest six co-channel cells in a cellular system with cluster size $N = 7$. The six interfering signals indicated on the diagram represent the case when the mobile is at the edge of the cell (this is often the worst-case as the desired signal is weakest).

2.2.2 Models for the Received Power

The *average* signal strength decreases with the separation distance, d , between the transmitter and receiver, and in outdoor environment can be approximated as

$$P_r = P_0 \left(\frac{d}{d_0} \right)^{-n} \quad (\text{W}) \quad (4)$$

where P_0 is the power received at a close reference distance d_0 in the far-field of the transmitter and n is the path-loss distance dependency exponent. In decibel units (4) can be written

$$P_r \text{ (dBm)} = P_0 \text{ (dBm)} - 10n \log_{10} \left(\frac{d}{d_0} \right). \quad (5)$$

Experimental measurements have shown the path-loss exponent is typically between 2–4 in outdoor environments. From (4) the SIR can be expressed in terms of distances between the mobile and desired and interfering base-stations. When the mobile is at the edge of a cell, the SIR is

$$SIR = \frac{R^{-n}}{C \sum_{i=1} D_i^{-n}} \quad (6)$$

where R is the radius of the cell and D_i is the distance between the mobile on the edge of the cell and the i -th co-channel base-station. If we consider only the first layer of interfering cells and approximate $D_i \approx D$, (6) can be simplified to

$$\begin{aligned} SIR &= \frac{(D/R)^n}{C} \\ &= \frac{(\sqrt{3N})^n}{C}. \end{aligned} \quad (7)$$

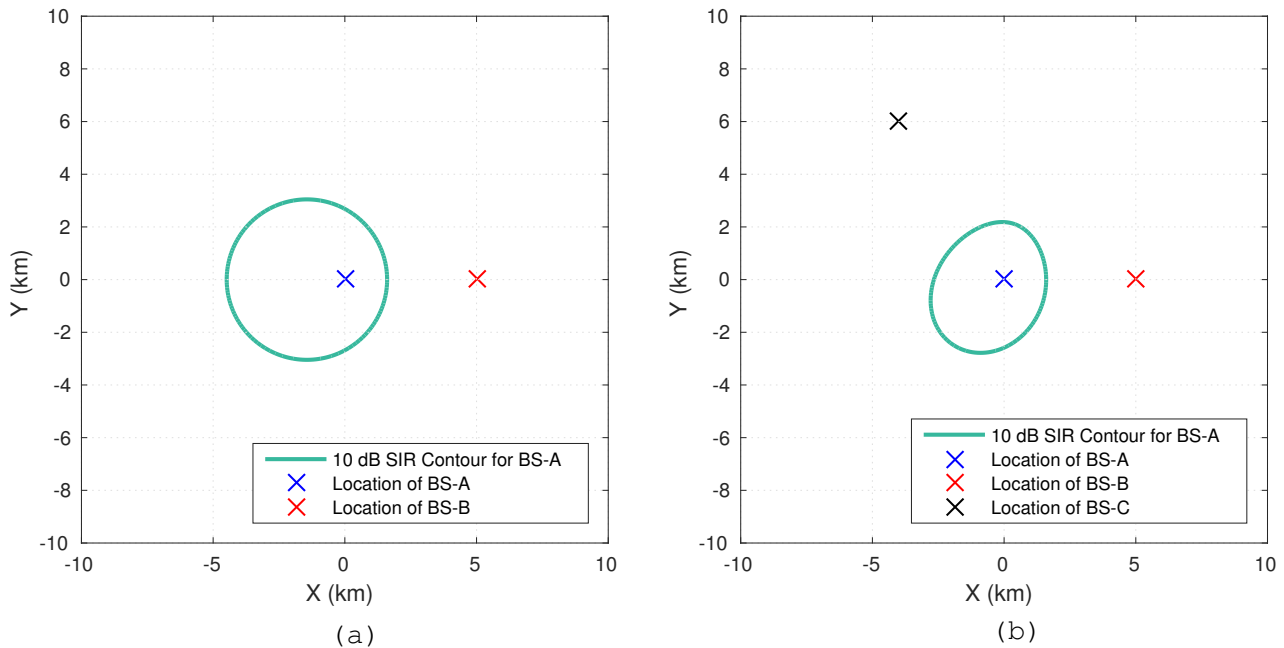


Fig. 11: (a) 10 dB SIR contour for BS-A with one co-channel base-station (BS-B); (b) 10 dB SIR contour for BS-A with two co-channel base-station (BS-B and BS-C).

This expression relates the SIR to the cluster size. Most wireless systems require a minimum SIR in order to operate correctly, for example, in the 1G AMPS system subjective tests indicated sufficient voice quality could be provided when $SIR > 18$ dB [1, p. 39]. In digital systems, decreasing the SIR leads to increased bit-error-rates, similar to the performance in the presence of noise. If the SIR criterion is not met, the system will experience an *outage*.

2.2.3 SIR Contours

In general, the SIR varies across the cell (the derivation above represents the worse-possible-case, where the user is at the edge of a cell). In particular, when the co-channel interfering base-stations are not arranged in to a regular hexagonal grid, the SIR must be calculated using (3) directly. We can thus determine *SIR contours* that represent the region around a base-station where the SIR is equal to some value. For example, Fig. 11(a) shows the 10 dB SIR contour around the desired base-station A, when the (only) co-channel interfering base-station is located 5 km away (at point B). In this case, it is assumed that base-station B transmits *twice* the power of base-station A. At any point within the contour, the (average) SIR exceeds 10 dB. Note, that while the SIR contour is circular it is not centred on base-station A. Fig. 11(b) shows the distortion in the 10 dB SIR contour when an additional co-channel base-station is introduced.

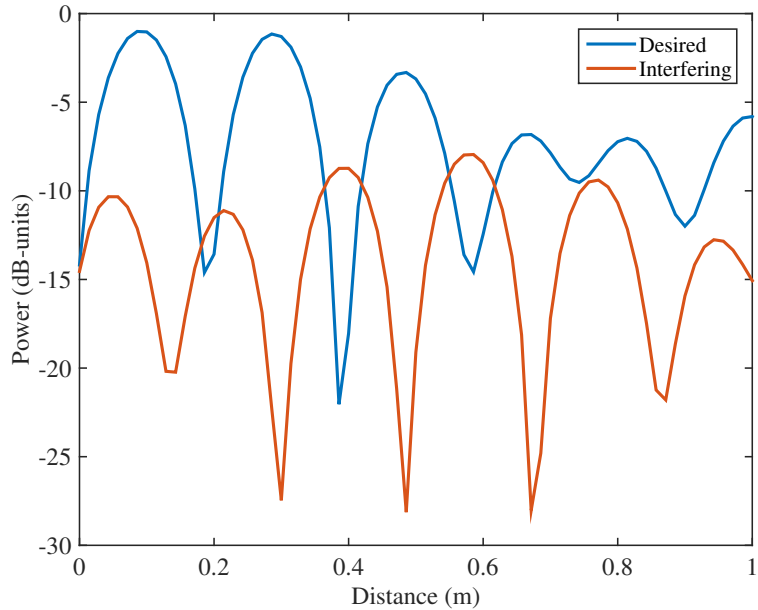


Fig. 12: Multipath fading at 1.7 GHz over a 1 m distance.

2.3 Outage Probability

2.3.1 Impact of Fading

The discussion about SIR in the previous section only considered the *average* signal power. However, due to multipath fading in the environment the instantaneous power of the signals can vary significantly as the receiver is moved. Fig. 12 shows the variations in signal level experienced as a receiver is moved over a 1 m distance (the frequency of operation is 1.7 GHz). The *average* SIR between the desired and interfering signals is 10 dB, however it is clear that even over a 1 m distance the *instantaneous* SIR is often less than 10 dB (and in some cases is negative, i.e., the interference is stronger than the desired signal!).

2.3.2 Rayleigh Fading

In order to determine when (and in particular how often) the instantaneous SIR drops below the threshold for suitable service, we need to consider suitable models for multipath fading. For typical outdoor cellular radio channels, the line-of-sight path between the transmitting and receiving antennas is often blocked, and energy tends to arrive via scattered paths. Accordingly, we can approximate the *time-harmonic* electric field¹² at the receiving antenna, $E(\mathbf{r})$ as a superposition of I plane waves arriving at

¹²Note that in general this is also a vector field.

arbitrary angles, i.e.,

$$E(\mathbf{r}) = \sum_{i=1}^I E_i e^{-j\mathbf{k}_i \cdot \mathbf{r}} \quad (8)$$

where \mathbf{r} is the observation point, E_i is the (complex) amplitude of the i -th plane wave, and \mathbf{k}_i is the wave-vector of the i -th plane wave, given by

$$\mathbf{k}_i = k_0 [\cos(\phi_i) \sin(\theta_i) \hat{x} + \sin(\phi_i) \sin(\theta_i) \hat{y} + \cos(\phi_i) \hat{z}] \quad (9)$$

where $k_0 = \frac{2\pi}{\lambda}$ is the wave number, and ϕ_i and θ_i are the azimuth and elevation angles of the i -th component. It has been observed that the azimuth angle of the components is uniformly distributed in scattering environments. Note that the angle of arrival in the elevation plane, θ , is usually restricted to 90° as previous analysis of outdoor cellular radio channels has indicated the majority of the energy arrives only slightly above or below the horizon.

If there are a sufficiently large enough number of components, it can be assumed via the central limit theorem that E_i is complex Gaussian distributed, i.e., the real and imaginary parts of E_i are *independently* Gaussian distributed. The aim is to find the resulting probability distribution of the signal envelope, R , given by

$$R = \sqrt{X_1^2 + X_2^2} \quad (10)$$

where X_1 and X_2 are independently Gaussian distributed, i.e.,

$$X_1 \sim N(0, \sigma^2) \quad (11)$$

$$X_2 \sim N(0, \sigma^2). \quad (12)$$

It can be shown (in Appendix A) that the PDF of R is

$$P_R(r) = \frac{r}{\sigma^2} \exp\left[-\frac{r^2}{2\sigma^2}\right] \quad (13)$$

for $r \geq 0$.

The Rayleigh distribution (113) describes the statistics of the variation in time-harmonic electric field as we move the receiving antenna in a scattered multipath environment with no line-of-sight component. Note that this is measured in units of Volts (strictly speaking this is Volts/m). The Rayleigh distribution is a *single-parameter* distribution, i.e., all information about the statistics of R can be determined from σ . The mean of a Rayleigh distribution is given by

$$\mu(R) = \sigma \sqrt{\frac{\pi}{2}}. \quad (14)$$

Fig. 13 shows probability density functions (PDF) for Rayleigh distributions with $\sigma = 0.5$ and $\sigma = 2.0$.

2.3.3 Rician Fading

It should be noted that there are many other statistical models for the multipath fading and shadowing envelope. In particular, when a dominant

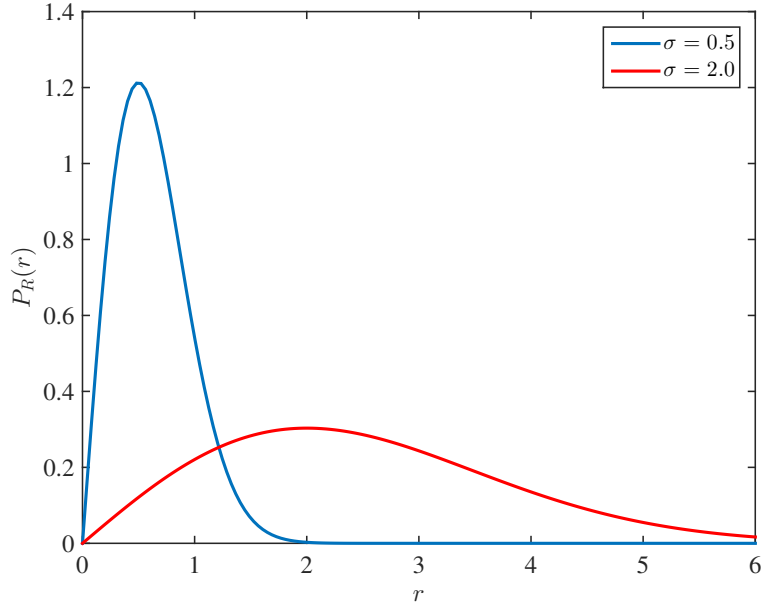


Fig. 13: PDFs of the Rayleigh distribution with $\sigma = 0.5$ and $\sigma = 2.0$.

component (usually in a radio channel, this is the line-of-sight path) exists, the PDF of the fading envelope follows a *Rician* distribution, given¹³ by

$$P_R(r) = \frac{r}{\sigma^2} \exp\left[-\frac{(r^2 + \nu^2)}{2\sigma^2}\right] I_0\left(\frac{r\nu}{\sigma^2}\right) \quad (15)$$

where ν represents the strength of the dominant component, and $I_0(\cdot)$ is the modified Bessel function of the first kind with order 0. The Rician K -factor (in linear units) is given by

$$K = \frac{\nu^2}{2\sigma^2} \quad (16)$$

and represents the relative strength of the power carried on the line-of-sight path to all the other multipath components (which are assumed to be uniformly distributed in angle-of-arrival). Note that as $K \rightarrow 0$, the Rician distribution degenerates to a Rayleigh distribution.

2.3.4 Variable Transformations

Often we want to determine the probability distribution *after* applying some transformation to the received signal. This is typically encountered in wireless systems when converting from voltage to power, or when expressing power in linear (Watts) or logarithmic (dB) units. Fig. 14 graphically illustrates this procedure: we know the PDF of the variable x , given by $P_X(x)$,

¹³Eqn (15) can be derived similarly to the Rayleigh PDF, by assuming the variables X_1 and X_2 in (11)–(12) have a mean value, ν .

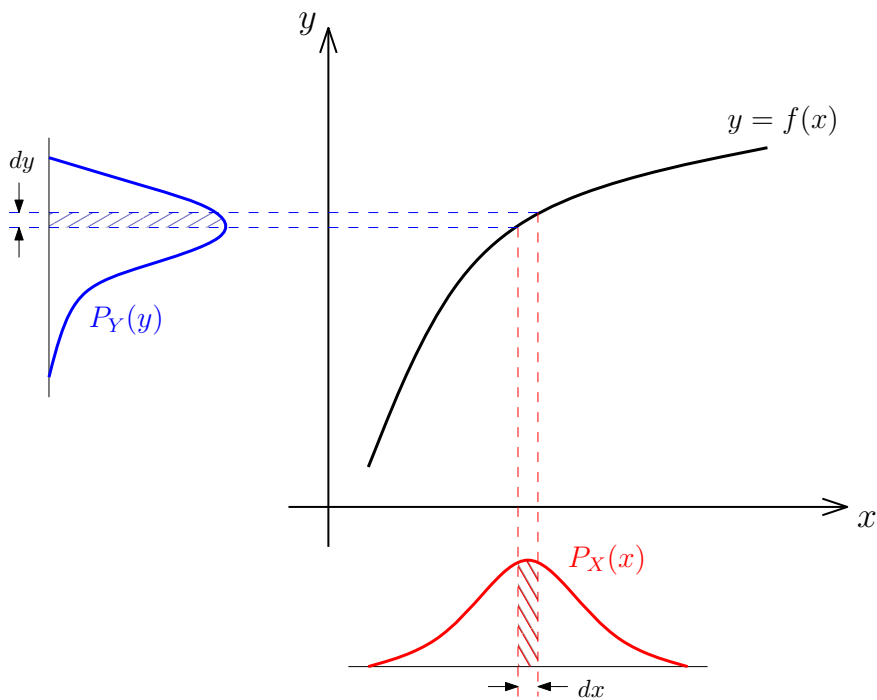


Fig. 14: Graphical illustration of how the probability distribution $P_Y(y)$ is estimated from $P_X(x)$ when $y = f(x)$.

we wish to determine the probability distribution of y , $P_Y(y)$, knowing that $y = f(x)$.

As probability is conserved during the mapping from x to y the probability of finding Y in the differential range dy must be equal to the probability of finding X in the differential range dx , i.e.,

$$P_Y(y) |dy| = P_X(x) |dx| \quad (17)$$

therefore,

$$P_Y(y) = P_X(x) \left| \frac{dx}{dy} \right| \quad (18)$$

where the absolute values are required to ensure non-negative probabilities.

From (113) we know that the voltage envelope, r , follows a Rayleigh distribution, what probability distribution does the power (in Watts), u , follow? To determine this, let

$$u = \frac{r^2}{2} \quad (19)$$

$$\text{thus } du = r dr \quad (20)$$

$$\frac{dr}{du} = \frac{1}{r}. \quad (21)$$

Hence,

$$P_U(u) = P_R(r) \left| \frac{dr}{du} \right| \quad (22)$$

$$= \frac{1}{\sigma^2} \exp \left[-\frac{u}{\sigma^2} \right]. \quad (23)$$

Eqn (23) describes an *exponential* probability distribution. Note that we assumed a 1Ω resistor when converting the voltage into power. The mean of (23) is σ^2 .

2.3.5 Outage Probability

Consider a desired signal, s , in the presence of one co-channel interfering signal i , assume that the desired signal experiences fading, while initially the interfering signal is a constant value. The probability that the desired signal, does **not** experience an outage (i.e., it is *serviced*) is

$$P_{ser} = 1 - P_{out} = \int_{r_p i}^{\infty} P_S(s) ds \quad (24)$$

where r_p is the receiver protection margin. Eqn (24) simply states that in order to find the probability the desired signal is serviced, we integrate the PDF of the desired signal $P_S(s)$ from r_p times the value of the interference i to infinity.

Now, i is *also* a random variable with probability distribution $P_I(i)$, so to find the actual probability of service we need to integrate over i , i.e.,

$$P_{ser} = \int_0^{\infty} P_I(i) \int_{r_p i}^{\infty} P_S(s) ds di. \quad (25)$$

In the general case, we also have $n = 1 \dots N$ co-channel interferers, if we assume that these are all independent, then the expression for the service probability is

$$P_{ser} = \int_0^{\infty} P_{I_1}(i_1) \int_0^{\infty} P_{I_2}(i_2) \int_0^{\infty} P_{I_3}(i_3) \dots \int_0^{\infty} P_{I_N}(i_N) \cdot \int_{r_p \sum_{n=1}^N i_n}^{\infty} P_S(s) ds di_N \dots di_3 di_2 di_1. \quad (26)$$

Note that in order for the desired signal to be received, it must exceed the sum of *all* the interfering signal (with the protection margin applied).

This **expression** appears unwieldy, but does actually converge to some simple, meaningful solutions: for example, consider a scenario where the desired signal and all N co-channel interferers are subject to Rayleigh fading¹⁴, i.e, the powers are exponentially distributed, as per (23), in this case, let

$$P_S(s) = \frac{1}{A} \exp \left(\frac{-s}{A} \right) \quad (27)$$

¹⁴What sort of environment are we assuming?

thus the inner most integral in (26) can be evaluated as

$$\int_{r_p \sum_{n=1}^N i_n}^{\infty} P_S(s) ds = \exp\left(\frac{-r_p \sum_{n=1}^N i_n}{A}\right) \quad (28)$$

$$= \exp\left(\frac{-I_1 r_p}{A}\right) \exp\left(\frac{-I_2 r_p}{A}\right) \exp\left(\frac{-I_3 r_p}{A}\right) \dots \exp\left(\frac{-I_N r_p}{A}\right) \quad (29)$$

and substituting this back in to (26) yields

$$P_{ser} = \int_0^{\infty} P_{I_1}(i_1) \exp\left(\frac{-i_1 r_p}{A}\right) \int_0^{\infty} P_{I_2}(i_2) \exp\left(\frac{-i_2 r_p}{A}\right) \int_0^{\infty} P_{I_3}(i_3) \exp\left(\frac{-i_3 r_p}{A}\right) \dots \int_0^{\infty} P_{I_N}(i_N) \exp\left(\frac{-i_N r_p}{A}\right) di_N \dots di_3 di_2 di_1. \quad (30)$$

Which can be simplified as

$$P_{ser} = \prod_{n=1}^N \int_0^{\infty} P_{I_n}(i_n) \exp\left(\frac{-i_n r_p}{A}\right) di_n. \quad (31)$$

As the interfering signals are also exponentially distributed, let

$$P_{I_n}(i_n) = \frac{1}{B_n} \exp\left(\frac{-i_n}{B_n}\right) \quad (32)$$

then the integral in (31) can be written as

$$\int_0^{\infty} P_{I_n}(i_n) \exp\left(\frac{-i_n r_p}{A}\right) = \int_0^{\infty} \frac{1}{B_n} \exp\left(\frac{-i_n}{B_n} \left[1 + \frac{B_n r_p}{A}\right]\right) di_n \quad (33)$$

$$= \frac{1}{1 + \frac{B_n r_p}{A}} \quad (34)$$

$$= \frac{\frac{A}{B_n}}{\frac{A}{B_n} + r_p}. \quad (35)$$

Thus, finally,

$$P_{ser} = \prod_{n=1}^N \frac{\Lambda_n}{\Lambda_n + r_p} \quad (36)$$

where $\Lambda_n = \frac{A}{B_n}$, i.e, the SIR for the n -th co-channel interferer. This is very significant result, as it implies the outage probability (when all our signals are subject to Rayleigh fading) *only* depends on the predictions of the mean signal strengths!

3 Space Diversity and MIMO

3.1 Diversity Transmission and Reception

Clearly multipath fading can have an extremely detrimental effect on the performance of a cellular system, particularly when considering co-channel interference. Diversity transmission and reception is an important technique for overcoming the impairments of the channel. The basic concept of diversity is that the receiver should have multiple ‘versions’ of the original signal, where each version was transmitted through a distinct channel. In general this can be achieved by using multiple transmitting antennas and/or receiving antennas. By appropriately spacing the antennas apart the fading experienced on each can be modelled as (largely) independent.

3.2 Selection Diversity

Fig. 15(a) shows the signals received on two antennas (approx 1 wavelength apart) in a multipath environment assuming Rayleigh fading. Note that at this stage we are still assuming a *single* transmitting antenna and no interfering signals (yet!). As expected there are significant variations in the power of the signal as we move the pair of antennas (maintaining the 1λ separation) in space. However, we observe that the fading patterns are largely *uncorrelated*, i.e., if antenna 1 experiences a deep fade, antenna 2 is likely to have a high(er) value, and vice versa. Fig. 15(b) shows the same result, but now assumes that we have the ability to switch our communications receiver to demodulate the signal from the strongest antenna. This approach is termed *selection diversity*.

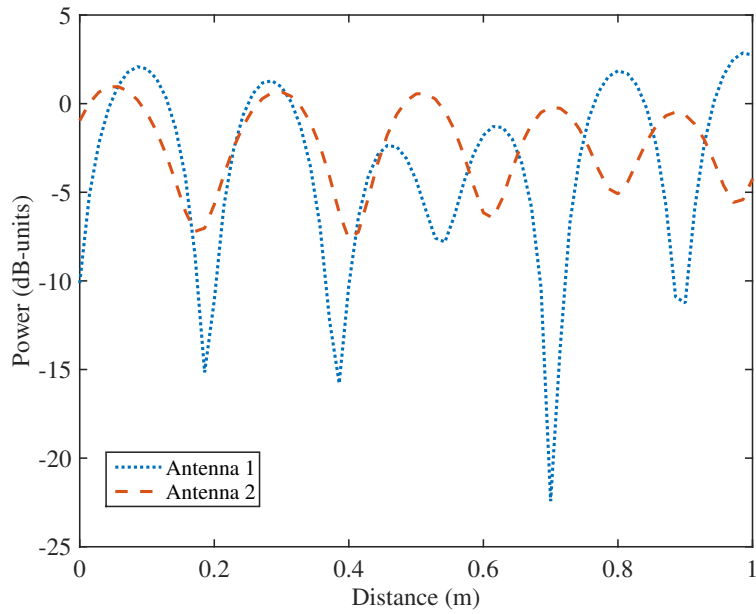
Fig. 16 shows the block diagram for a selection diversity system, with multiple receiving antennas. The underlying assumption is that we can monitor and switch the signal fast enough with little impact on the receiver circuitry. If all N branches have the same power, the amplitude of the output from the selection combiner is simply the maximum instantaneous signal across all the inputs. The probability that the signal level from the selection diversity combiner drops below some level γ due to fading is thus the product of individual probabilities for each branch, i.e.,

$$P_U(u_1, u_2, \dots, u_N < \gamma) = \prod_{n=1}^N P_U(u_n < \gamma) \quad (37)$$

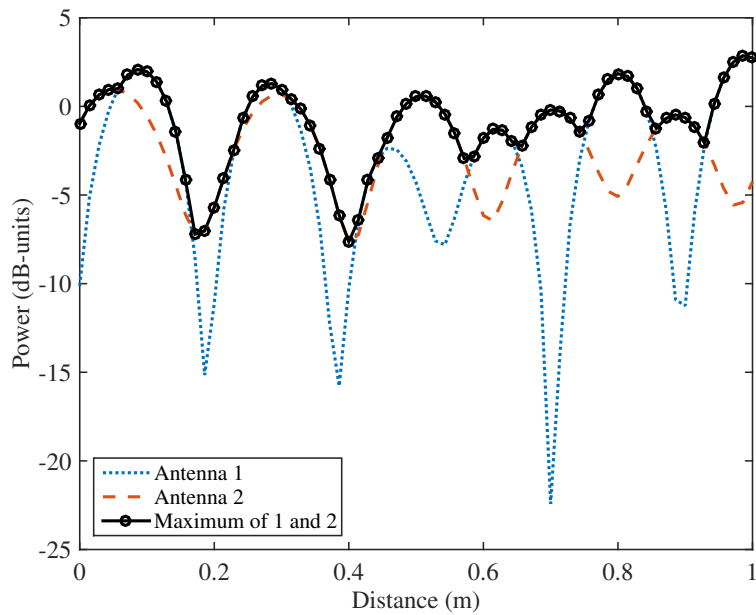
and assuming the PDFs for $P_U(u_n)$ are identical and Rayleigh distributed, yields

$$P_U(u_1, u_2, \dots, u_N < \gamma) = [1 - \exp(-\gamma)]^N. \quad (38)$$

Eqn (38) indicates that the probability of experiencing a ‘deep’ fade is significantly reduced as we increase the number of antennas in our selection diversity system. This is illustrated in Fig. 17 which plots the probability that the signal is less than the value on the x -axis (also called the *abscissa*). Note that diminishing returns are observed as we increase N , but that a significant *diversity gain* is experienced when introducing selection diversity.



(a)



(b)

Fig. 15: (a) Received signals on two antennas both subjected to Rayleigh fading; and (b) Same received signals, but assuming we can detect (and use) the maximum of the two.

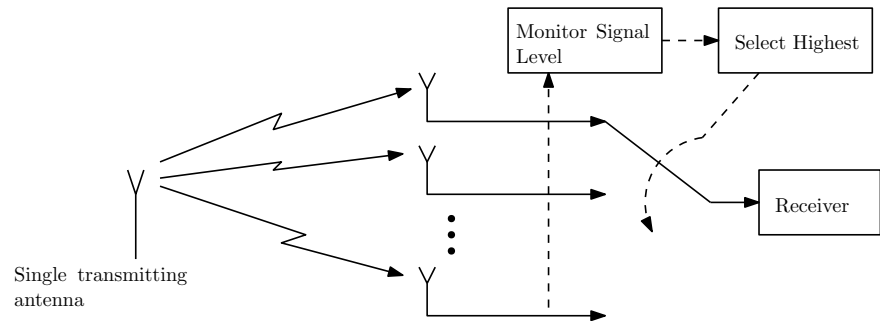


Fig. 16: Block diagram for a selection diversity combiner.

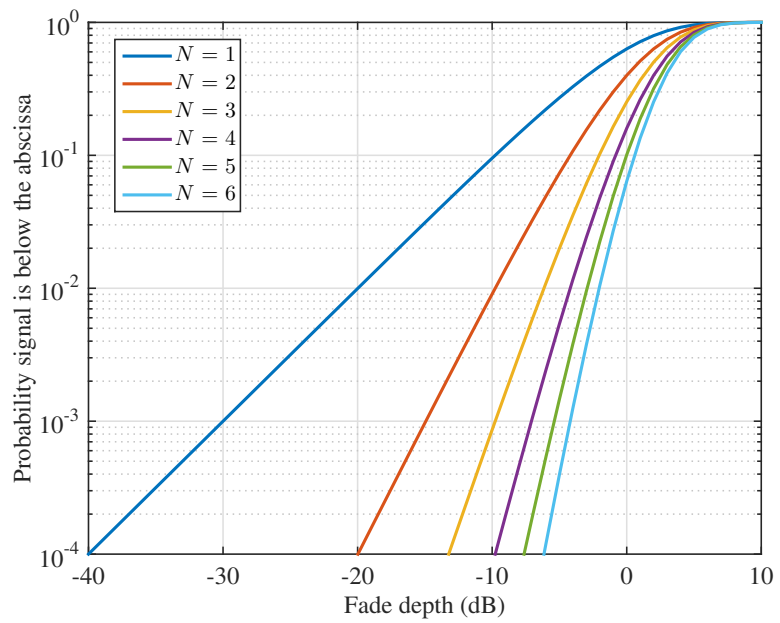


Fig. 17: Diversity gain for a selection combiner.

3.2.1 Outage Probability

For an ideal N -branch selection diversity receiver, outage only occurs when *all* branches are in a state of outage. If we assume the fading received on each branch is independent (we will revisit this assumption in the next section), and that the probability of outage on a single branch is $P_{out-branch}$, then

$$P_{out-diversity} = [P_{out-branch}]^N. \quad (39)$$

For an exponentially distributed desired signal

$$P_{out-branch} = \int_0^{x_{min}} \frac{1}{A} \exp\left(\frac{-x}{A}\right) dx \quad (40)$$

$$= 1 - \exp\left(\frac{-x_{min}}{A}\right). \quad (41)$$

Hence

$$P_{out-diversity} = \left[1 - \exp\left(\frac{-x_{min}}{A}\right)\right]^N. \quad (42)$$

Example—Diversity Gain

The diversity gain (in dB) for a two-branch selection diversity system relative to a single branch (non-diversity) system can be computed, but we need to assume an outage probability level. In this case we use 1%:

For a single branch system:

$$P_{out-branch} = 1 - \exp\left(\frac{-x_{min}}{A_1}\right) = 0.01 \quad (43)$$

$$\therefore \frac{A_1}{x_{min}} = 99.5 \quad (44)$$

For a two-branch system:

$$P_{out-branch} = 1 - \exp\left(\frac{-x_{min}}{A_2}\right) = \sqrt{P_{out-diversity}} = 0.1 \quad (45)$$

$$\therefore \frac{A_2}{x_{min}} = 9.491 \quad (46)$$

Hence the diversity gain (at 1% outage probability) is

$$\frac{A_1}{A_2} = \frac{A_1}{x_{min}} \frac{x_{min}}{A_2} \quad (47)$$

$$= \frac{99.5}{9.491} = 10.48 \equiv 10.2 \text{ dB} \quad (48)$$

This result implies we can operate a two-branch selection diversity system with an input power 10.2 dB *lower* than a single-branch system and still maintain 1% outage probability.

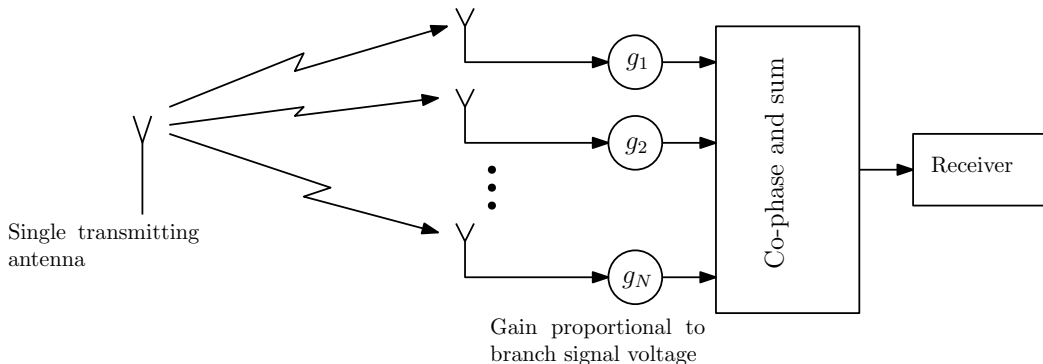


Fig. 18: Block diagram for a MRC diversity combiner.

3.3 Maximal-Ratio-Combining Diversity Systems

Fig. 18 shows the block diagram of a maximal-ratio-combining (MRC) diversity scheme. In MRC diversity the signal voltage on each branch is scaled in proportion to its magnitude and *co-phased* before being added. The gains g_1, g_2, \dots, g_N must be adaptively controlled as the voltages on each branch change as the antennas are moved in space¹⁵. For a two-branch MRC diversity system, the voltage sum of the two scaled branch signal voltages, S_{v1} and S_{v2} after co-phasing is given by

$$V_s = S_{v1} (S_{v1}) + S_{v2} (S_{v2}). \quad (49)$$

The power of the output signal is thus

$$P_s = (S_{v1}^2 + S_{v2}^2)^2. \quad (50)$$

Note that we also have (independent) noise present on each branch. Typically we model the noise as an additive Gaussian random process (we also assume the spectrum is flat or “white”). It would appear that MRC diversity would not help improve the signal-to-noise ratio (SNR), as the noise voltage on each branch will also be scaled by the same factor as the signal. However, the phase angle of the noise is random, thus when we co-phase the signals this will not co-phase the noise. Because the noise phasors are not co-phased they will add on a *power basis* rather than voltage basis. For example, consider two phasors A and B , with a random angle between them θ (what distribution should θ follow?), as depicted in Fig. 19.

The *average* magnitude of the resultant C is thus

$$E \{C^2\} = E \{A^2 + B^2 - 2AB \cos \theta\} \quad (51)$$

$$= E \{A^2 + B^2\} - E \{2AB \cos \theta\} \quad (52)$$

$$= E \{A^2 + B^2\} \quad (53)$$

$$= A^2 + B^2. \quad (54)$$

¹⁵In the case where the antennas are fixed in position, e.g., a base-station the voltages will change as the mobile transmitter moves in space.

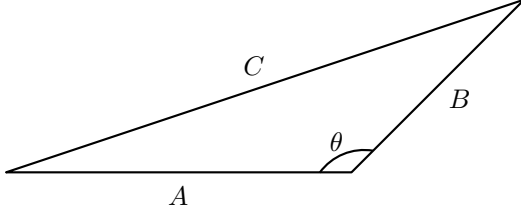


Fig. 19: The cosine rule.

Applying this result to the noise voltage n_v leads to the following expression for the noise power, P_n

$$P_n = (n_v S_{v1})^2 + (n_v S_{v2})^2 \quad (55)$$

$$= n_v^2 (S_{v1}^2 + S_{v2}^2). \quad (56)$$

Hence the SNR at the output of the MRC diversity system is

$$SNR = \frac{P_s}{P_n} = \frac{(S_{v1}^2 + S_{v2}^2)^2}{n_v^2 (S_{v1}^2 + S_{v2}^2)} \quad (57)$$

$$= \frac{S_{v1}^2 + S_{v2}^2}{n_v^2} \quad (58)$$

$$= \frac{S_{v1}^2}{n_v^2} + \frac{S_{v2}^2}{n_v^2} \quad (59)$$

which is the *sum* of the SNRs on each branch, i.e., MRC diversity leads to an overall increase in the SNR.

3.3.1 Outage Probability

The outage probability of a two branch MRC diversity system, with exponentially distributed signal power is given by

$$P_{out} = \int_0^{x_{min}} \frac{1}{A} \exp\left(\frac{-x_1}{A}\right) \int_0^{x_{min}-x_1} \frac{1}{A} \exp\left(\frac{-x_2}{A}\right) dx_2 dx_1 \quad (60)$$

where A is the mean power of the signal and x_{min} is the minimum signal required for adequate reception.

To find a closed form expression for the outage probability in this case, we need to first evaluate the inner integral, yielding

$$\int_0^{x_{min}-x_1} \frac{1}{A} \exp\left(\frac{-x_2}{A}\right) dx_2 dx_1 = \exp\left(\frac{-x_2}{A}\right) \Big|_{x_{min}-x_1}^0 \quad (61)$$

$$= 1 - \exp\left(\frac{x_1 - x_{min}}{A}\right) \quad (62)$$

Therefore,

$$P_{out} = \int_0^{x_{min}} \frac{1}{A} \exp\left(\frac{-x_1}{A}\right) \left[1 - \exp\left(\frac{x_1 - x_{min}}{A}\right)\right] dx_1 \quad (63)$$

$$= \int_0^{x_{min}} \frac{1}{A} \exp\left(\frac{-x_1}{A}\right) - \frac{1}{A} \exp\left(\frac{-x_{min}}{A}\right) dx_1 \quad (64)$$

$$= 1 - \exp\left(\frac{-x_{min}}{A}\right) - \frac{x_{min}}{A} \exp\left(\frac{-x_{min}}{A}\right) \quad (65)$$

$$= 1 - \exp\left(\frac{-x_{min}}{A}\right) \left[1 + \frac{x_{min}}{A}\right]. \quad (66)$$

Example—Diversity Gain

Similar to section 3.2.1, we can compute the diversity gain for an MRC scheme (relative to a single-branch system) by assuming an outage probability level of 1%:

For a 1% outage probability:

$$\exp\left(\frac{-x_{min}}{A}\right) \left[1 + \frac{x_{min}}{A}\right] = 0.99 \quad (67)$$

This expression does need to be solved numerically, doing so we find

$$\frac{A}{x_{min}} = \frac{1}{0.14855} \quad (68)$$

$$= 6.73 \quad (69)$$

From the previous example, for a single branch system:

$$P_{out-branch} = 1 - \exp\left(\frac{-x_{min}}{A_1}\right) = 0.01 \quad (70)$$

$$\therefore \frac{A_1}{x_{min}} = 99.5 \quad (71)$$

The diversity gain is thus

$$\frac{A_1}{A} = 14.79 \equiv 11.7 \text{ dB}. \quad (72)$$

3.4 Assumptions for Diversity Reception

In the analysis of diversity selection/combining we made the assumption that the signals received on each of the N branches were statistically independent. Another way of stating this is that the *correlation* between branch is zero. The correlation between the field recorded at two antennas separated in space depends on both the propagation environment (it must be *sufficiently scattering*) and the separation distance between the antennas.

To analyse the impact of the separation distance, we can set up a highly simplified geometry and use plane-waves to estimate the correlation between

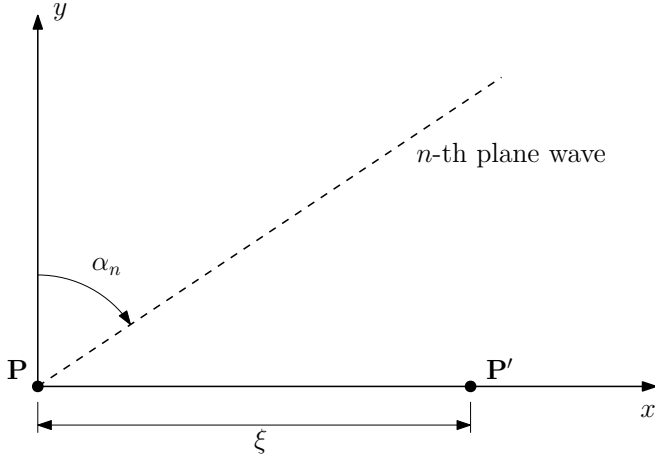


Fig. 20: Plane wave geometry for two antennas separated by distance ξ .

two antennas. This geometry is shown in Fig. 20, where the electric field is assumed to be vertically polarised, the two antennas are separated by a distance ξ , and N plane-waves are incident. Note that we are not yet making any assumptions of the arrival angles, α . The phase difference, ϕ between the fields incident on the antennas for each component is thus

$$\phi_n = -k\xi \sin \alpha_n. \quad (73)$$

Where there are a large number of components, the total field at \mathbf{P}' can be written

$$E_{\mathbf{P}'} = \sum_{n=1}^N e_n \quad (74)$$

where e_n is the amplitude of each component, while the total field at \mathbf{P} is

$$E_{\mathbf{P}} = \sum_{n=1}^N e_n \exp(j\phi_n). \quad (75)$$

The correlation, R between $E_{\mathbf{P}}$ and $E_{\mathbf{P}'}$ is thus

$$R = E \left\{ \sum_{n=1}^N e_n \exp(-j\phi_n) \right\} \quad (76)$$

$$= E \left\{ \sum_{n=1}^N e_n \exp(k\xi \sin \alpha_n) \right\}. \quad (77)$$

As α is a random variable, we can find R by integrating over the PDF, i.e.,

$$R(\xi) = \int_0^{2\pi} P(\alpha) \exp(k\xi \sin \alpha) d\alpha. \quad (78)$$

Note that this is essentially a Fourier integral, which implies a narrow distribution of arrival angle leads to a ‘slow’ variation in R (which limits the

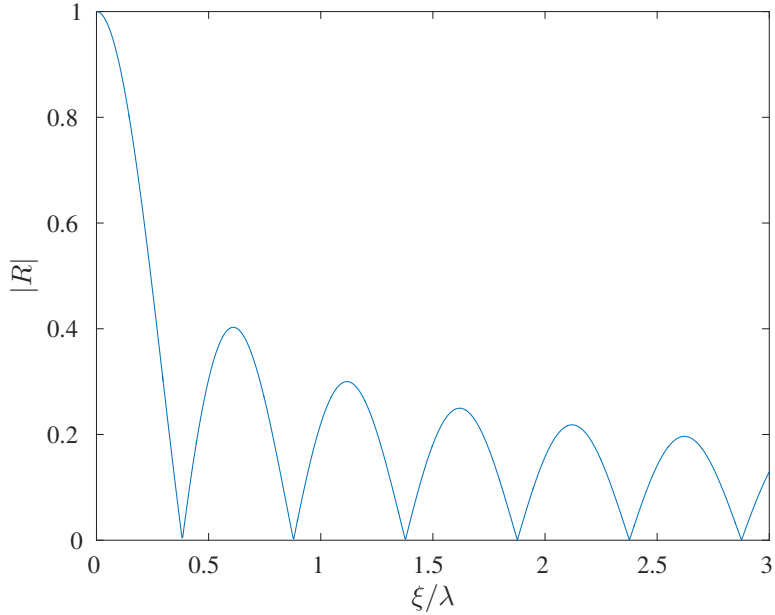


Fig. 21: Correlation in the received field for two antennas separated by distance ξ .

use of diversity), while environments that scatter the energy lead to smaller values of R . In the case when α is uniformly distributed over $[0 - 2\pi]$, the correlation reduces to

$$R(\xi) = J_0(k\xi), \quad (79)$$

where J_0 is the zero-th order Bessel function of the first kind. Eqn 79 is plotted in Fig. 21, showing that the correlation coefficient tends to decrease with increasing ξ (there are also null-points, where it is exactly zero). Measured correlation coefficients in macro-cellular environments follow a similar trend.

3.5 Multiple-Input Multiple Output (MIMO) Systems

MIMO extends the ideas of diversity reception to the transmitter side. As depicted in Fig. 22, a general MIMO system consists of N_t transmit antennas and N_r receiving antennas, note that N_t does not have to be equal to N_r , though it often is in practise. Unlike a diversity system, where there is only a single ‘receiver’ block, in MIMO we typically have a complete receiver chain (i.e., antenna, amplifier, down-converter, and analog-to-digital converter) for each branch. This increases the cost and power consumption of MIMO systems, but allows the application of digital signal processing to separate out the different signal streams.

Taking only the first receiver branch, the received voltage, y_1 is thus

$$y_1 = h_{11}x_1 + h_{12}x_2 + \dots + h_{1N_t}x_{N_t} \quad (80)$$

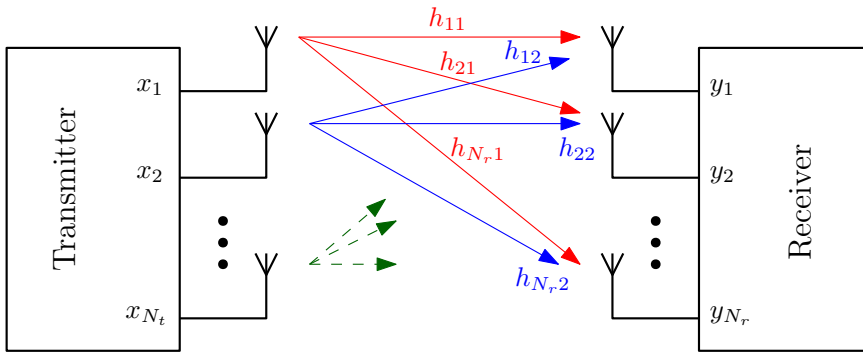


Fig. 22: Generalised MIMO system, where h_{nm} represents the (complex) radio channel between transmitter n and receiver m .

where $x_1 \dots x_{N_t}$ are the ‘input’ voltages at the transmitting antennas, and h_{rt} represents the (complex) radio channel between the t -th transmitter and r -th receiver. Eqn (80) describes a multiple-input single-output (MISO) system. Similarly, taking only the first transmitter branch, the expressions for the N_r receiver branches would be

$$y_1 = h_{11}x_1 \quad (81)$$

$$y_2 = h_{21}x_1 \quad (82)$$

\vdots

$$y_{N_r} = h_{N_r,1}x_1. \quad (83)$$

Eqns (81)–(83) describe a single-input multiple-output system (SIMO), which is very similar to reception diversity analysed in the previous section.

In the general case, if we transmit on N_t antennas simultaneously, the received signals are

$$y_1 = h_{11}x_1 + h_{12}x_2 + \dots + h_{1N_t}x_{N_t} \quad (84)$$

$$y_2 = h_{21}x_1 + h_{22}x_2 + \dots + h_{2N_t}x_{N_t} \quad (85)$$

\vdots

$$y_{N_r} = h_{N_r,1}x_1 + h_{N_r,2}x_2 + \dots + h_{N_r,N_t}x_{N_t}. \quad (86)$$

This can be expressed more simply in matrix form as

$$\begin{bmatrix} y_1 \\ y_2 \\ \vdots \\ y_{N_r} \end{bmatrix} = \begin{bmatrix} h_{11} & h_{12} & \dots & h_{1N_t} \\ h_{21} & h_{22} & \dots & h_{2N_t} \\ \vdots & \vdots & \ddots & \vdots \\ y_{N_r,1} & h_{N_r,2} & \dots & h_{N_r,N_t} \end{bmatrix} \begin{bmatrix} x_1 \\ x_2 \\ \vdots \\ x_{N_t} \end{bmatrix} \quad (87)$$

$$\mathbf{y} = \mathbf{H}\mathbf{x}. \quad (88)$$

The performance of a MIMO system depends on the channel matrix \mathbf{H} . While for diversity systems, we were most interested in reducing the impact

of fading to improve the coverage region from urban macro- and micro-cells, in MIMO systems the aim is typically to improve the *capacity* of the channel. Hence, MIMO is typically used in environments where base-stations/access-points are placed close together so there is sufficient coverage, but there is a need to support high data-rates, e.g., urban pico-cells and WiFi deployments within buildings.

MIMO works fundamentally by solving (88), given that we receive the signal \mathbf{y} . This implies that we have knowledge of the channel matrix \mathbf{H} . However, as this depends entirely on the fading environment, in general we do not, and it needs to be estimated. Typically the channel is estimated by periodically sending known training data, and assuming the channel stays static for a short period afterwards.

In general, unique solutions to (88) can only be found if the rows in \mathbf{H} are independent, i.e., uncorrelated. In MIMO systems, if there is sufficient multipath scattering in the channel the elements in the channel matrix, representing the individual channels between each pair of transmitter and receiving antennas become *decorrelated*. This means that we essentially have $\min\{N_t, N_r\}$ independent channels, through which we can send a separate data stream, thereby increasing the overall capacity of the link.

4 Wireless System Performance Estimation

In the previous sections we examined the impact of multipath fading on the quality of service in cellular systems, leading to expressions for the outage probability in the presence of co-channel interference and the improvements that can be made through diversity reception. In all of these cases we assumed the local variation of the signal followed a Rayleigh distribution. While the Rayleigh distribution is a good approximation of the multipath fading envelope in regions where there is no LOS path between the transmitter and receiver, other propagation effects are also important. In particular, for outdoor environments electrically large objects, such as buildings or hills, can cast radio shadows over significant distances, causing fluctuations in the sector mean over the medium-range (50–100 m); this phenomena is termed *shadowing*.

4.1 Lognormal Shadowing

The power of the shadowing signal¹⁶ has been observed to follow a *lognormal* distribution (when measured in linear units, i.e., Watts). A lognormal distribution for the power in linear units implies that the power follows a *Gaussian* distribution when measured in dB units. *Unlike Rayleigh fading, there is no rigorous electromagnetic explanation for why the PDF of shadowing follows a lognormal distribution.* However, lognormal shadowing has been repeatedly observed in experimental measurements of outdoor and indoor radio channels and regardless of its source, needs to be included to ensure accurate predictions of the outage probability.

4.1.1 Probability Density Function

When measured in dB units, the power of the shadowing component follows a Gaussian distribution, given by

$$P_X(x) = \frac{1}{\sqrt{2\pi}\sigma} \exp\left(\frac{-(x-m)^2}{2\sigma^2}\right) \quad (89)$$

where m represents the mean level of the signal (in dB units) and σ is the standard deviation, also measured in dB units. To determine the PDF of the signal in linear units, we need to apply a variable transform: let

$$u = 10^{\frac{x}{10}} \quad (90)$$

$$= \exp\left(\frac{x}{10} \ln(10)\right) \quad (91)$$

¹⁶Note that we typically extract the shadowing component by low-pass filtering the received signal to remove Rayleigh fading.

Hence

$$du = \frac{\ln(10)}{10} \exp\left(\frac{x}{10} \ln(10)\right) dx \quad (92)$$

$$\frac{dx}{du} = \frac{10}{\ln(10)} \exp\left(\frac{-x}{10} \ln(10)\right) \quad (93)$$

$$= \frac{10}{\ln(10)} 10^{\frac{-x}{10}}. \quad (94)$$

Thus,

$$P_U(u) = P_X(x) \left| \frac{dx}{du} \right| \quad (95)$$

$$= \frac{10}{\ln(10)} \frac{1}{u} \frac{1}{\sqrt{2\pi}\sigma} \exp\left(\frac{-(10 \log_{10}(u) - m)^2}{2\sigma^2}\right). \quad (96)$$

Eqn (96) is the PDF of the resulting lognormal distribution when the power is measured in linear units. Note that while (96) has two parameters (m and σ) these are *not* the mean and standard deviation of the lognormal distribution—they are the mean and standard deviation of the corresponding normal distribution from (89) and are in dB units.

4.2 Combining Rayleigh Fading with Lognormal Shadowing—The Suzuki Distribution

In urban macro- and micro-cellular channels we can model the *total* received signal power as a lognormal distribution—representing the variations in the mean signal level caused by shadowing—*superimposed* with an exponential distribution to represent multipath fading. The probability distribution that describes this case is called the *Suzuki* distribution and is given by

$$P_W(w) = \int_0^\infty \frac{10}{\ln 10} \frac{1}{A} \frac{1}{\sqrt{2\pi}\sigma} \exp\left[\frac{-(10 \log_{10}(A) - m)^2}{2\sigma^2}\right] \frac{1}{A} \exp\left[\frac{-w}{A}\right] dA \quad (97)$$

where we are essentially multiplying the PDFs of the exponential and lognormal distributions and taking the integral over the mean values of the exponential PDF. Note that there is no closed form expression for the Suzuki PDF, and it must be evaluated numerically.

4.2.1 Outage Probability for Multiple Suzuki Interferers

Note that the expression for the outage probability derived in (26) did not make any assumptions about the PDFs. For N Suzuki distributed interfering signals, we can substitute (97) into (26) (repeated here for convenience),

$$P_{ser} = \int_0^\infty P_{I_1}(i_1) \int_0^\infty P_{I_2}(i_2) \int_0^\infty P_{I_3}(i_3) \dots \int_0^\infty P_{I_N}(i_N) \\ \cdot \int_{r_p \sum_{n=1}^N i_n}^\infty P_S(s) ds di_N \dots di_3 di_2 di_1.$$

It can be shown (in Appendix B) that the resulting expression for the service probability is given by

$$P_{ser} = \frac{1}{\sqrt{\pi}} \int_{-\infty}^{+\infty} \exp(-y_0^2) \prod_{n=1}^N \left[\frac{1}{\sqrt{\pi}} \int_{-\infty}^{+\infty} \exp(-y_n^2) \frac{1}{1 + 10^{\frac{\sqrt{2}(\sigma_n y_n - \sigma_0 y_0) - \tau_n}{10}}} dy_n \right] dy_0 \quad (98)$$

where

$$y_n = \frac{10 \log_{10}(A_n) - m_n}{\sqrt{2} \sigma_n} \quad (99)$$

$$\text{and } \tau_n = m_0 - (m_n + 10 \log_{10}(r_p)). \quad (100)$$

This is still not a closed form expression, but can be readily computed using *Hermite Quadrature*.

Appendix A—derivation of Rayleigh probability distribution

Let

$$V = \arctan\left(\frac{X_2}{X_1}\right) \quad (101)$$

$$\text{thus } X_1 = R \cos V \quad (102)$$

$$\text{and } X_2 = R \sin V. \quad (103)$$

The joint distribution for R and V is given by

$$P_{R,V}(r, v) = P_{X_1, X_2}(x_1, x_2) \det [J(r, v)] \quad (104)$$

where $\det [J(r, v)]$ is the determinant of the Jacobian matrix, given by

$$\det [J(r, v)] = \begin{vmatrix} \frac{\partial x_1}{\partial r} & \frac{\partial x_1}{\partial v} \\ \frac{\partial x_2}{\partial r} & \frac{\partial x_2}{\partial v} \end{vmatrix} \quad (105)$$

$$= \begin{vmatrix} \cos v & r \sin v \\ \sin v & r \cos v \end{vmatrix} \quad (106)$$

$$= r (\cos^2 v + \sin^2 v) \quad (107)$$

$$= r. \quad (108)$$

As X_1 and X_2 are independent, the joint distribution P_{X_1, X_2} is given by

$$P_{X_1, X_2} = P_{X_1} P_{X_2} \quad (109)$$

$$= \frac{1}{2\pi\sigma^2} \exp\left[-\frac{x_1^2 + x_2^2}{2\sigma^2}\right]. \quad (110)$$

Thus

$$P_{R,V}(r, v) = \frac{r}{2\pi\sigma^2} \exp\left[-\frac{r^2}{2\sigma^2}\right]. \quad (111)$$

The PDF of R is

$$P_R(r) = \int_0^{2\pi} P_{R,V}(r, v) dv \quad (112)$$

$$= \frac{r}{\sigma^2} \exp\left[-\frac{r^2}{2\sigma^2}\right] \quad (113)$$

for $r \geq 0$.

References

- [1] T. Rappaport, *Wireless Communications Principles and Practice*, 1st ed. New Jersey: Prentice-Hall, 1996.
- [2] K. W. Sowerby, “Outage probability in mobile radio systems,” Ph.D. dissertation, The University of Auckland, Auckland, New Zealand, 1989.
- [3] N. Chandran and M. C. Valenti, “Three generations of cellular wireless systems,” *IEEE potentials*, vol. 20, no. 1, pp. 32–35, 2001.
- [4] “IEEE 802.11-2007—part 11: Wireless LAN medium access control (MAC) and physical layer (PHY) specifications,” IEEE, 2007.
- [5] A. Osseiran, F. Boccardi, V. Braun, K. Kusume, P. Marsch, M. Maternia, O. Queseth, M. Schellmann, H. Schotten, H. Taoka *et al.*, “Scenarios for 5G mobile and wireless communications: the vision of the METIS project,” *IEEE Communications Magazine*, vol. 52, no. 5, pp. 26–35, 2014.
- [6] E. G. Larsson, O. Edfors, F. Tufvesson, and T. L. Marzetta, “Massive MIMO for next generation wireless systems,” *IEEE Communications Magazine*, vol. 52, no. 2, pp. 186–195, 2014.